ELSEVIER

Available online at www.sciencedirect.com

SCIENCE DIRECT®

Physica B 367 (2005) 223–228

PHYSICA B

www.elsevier.com/locate/physb

Structure and photoluminescence of Mn-passivated nanocrystalline ZnO:S thin films

Y.H. Tong[a,b], Q.X. Tang[c], Y.C. Liu[c,*], C.L. Shao[c], C.S. Xu[c], Y.X. Liu[c]

[a]*Key Laboratory of Excited State Processes, Changchun Institute of Optics, Fine Mechanics and Physics, Chinese Academy of Sciences, Changchun 130033, People's Republic of China*

[b]*Graduate School of the Chinese Academy of Sciences, People's Republic of China*

[c]*Center for Advanced Opto-electronic Functional Material Research, Northeast Normal University, Changchun 130024, People's Republic of China*

Received 11 May 2005; received in revised form 14 June 2005; accepted 14 June 2005

Abstract

Mn-passivated nanocrystalline ZnO:S thin films were fabricated by thermally oxidizing Mn-doped ZnS (ZnS:Mn) films prepared by electron beam evaporation. Mn was introduced to passivate the surface defects of ZnO and to improve the optical properties. X-ray diffraction (XRD) and photoluminescence (PL) spectra at 81.9 K indicated the S content in ZnO thin film gradually decreased with increasing annealing temperature. The fitted result of the temperature-dependent PL spectra in the range from 81.9 to 302.2 K showed that S dopant could broaden the optical band gap energy of ZnO. Room temperature PL spectra confirmed that the ultraviolet peak shifted to lower energy with the decrease of S content in the thin film because of the Burstein–Moss effect.

© 2005 Published by Elsevier B.V.

PACS: 78.66.Hf; 81.15.Jj; 81.40.Ef

Keywords: ZnO:S; Mn passivation; photoluminescence

1. Introduction

As a wide band gap ($E_g = 3.37\,eV$) semiconductor with large exciton binding energy (59 meV) [1], ZnO has attracted considerable attention for its potential optoelectronic applications in the ultraviolet (UV) range. Many different techniques, such as sputtering [2], pulsed laser deposition (PLD) [3], metal-organic chemical vapor deposition (MOCVD) [4], and molecular beam epitaxy (MBE) [5], have been used to prepare ZnO thin films. Efficient impurity incorporation including

*Corresponding author. Tel.: +86 431 5098803; fax: +86 431 5684009.

E-mail address: ycliu@nenu.edu.cn (Y.C. Liu).

0921-4526/$ - see front matter © 2005 Published by Elsevier B.V.
doi:10.1016/j.physb.2005.06.022

Mg and transition metals in ZnO has been carried out in order to obtain novel properties and broaden possible applications [6–9]. However, little attention has been paid to S doping in ZnO thin films because of the difference between the low stability of sulfur and the high growth temperature of ZnO. Sulfur has a much smaller electronegativity (2.58) than that of oxygen (3.44) and the atom radius of sulfur (1.09 Å) is much larger than that of oxygen (0.65 Å). The difference between S and O makes it possible to obtain some novel properties of ZnO via S doping. Yoo et al. [10] have reported that the band gap of ZnO could be tuned via S dopant. S impurities are also expected to increase the electrical conductivity of ZnO by supplying excess carriers [11]. In this paper, we report a simple method for preparing Mn-passivated ZnO:S thin films by thermal oxidation of ZnS:Mn thin films. Mn was introduced to the system in order to improve the optical properties of ZnO [12]. In addition, X-ray diffraction (XRD) and photoluminescence (PL) spectra have been used to investigate the effect of S doping on the structural and optical properties of the thin film.

2. Experimental procedures

ZnS:Mn films were deposited on Si (0 0 1) substrates by using an electron-beam evaporation system. The pressure of the growth chamber was kept at 1×10^{-3} Pa. Before the deposition, the substrates were pre-cleaned by the normal RCA method and then were bombarded by Ar ions for 10 min to remove the oxide layer at the surface of the substrates. The substrate temperature was kept at 200 °C. ZnS:Mn sintered target with 5% Mn concentration was used as evaporation source. After deposition, thermal oxidation of ZnS:Mn thin films was carried out in oxygen ambient at temperatures ranging from 200 to 700 °C for 1 h.

The crystal structures of the thin films were investigated by XRD spectra using a D/Mac-rA X-ray diffraction spectrometer (Rigaku) with the CuKα line of 1.54 Å. The PL spectra from 330 to 600 nm were excited using the 325 nm line of a 45 mW He–Cd laser.

3. Results and discussion

Fig. 1 shows XRD patterns of the as-grown ZnS:Mn thin film and the thin films annealed at different temperatures ranging from 200 to 700 °C. XRD spectra indicated that every thin film exhibited preferred orientation. The as-grown film showed a main diffraction peak at $2\theta = 28.9^\circ$, corresponding to the (1 1 1) diffraction of the zinc blende (ZB) ZnS. When ZnS:Mn thin films were annealed in temperature ranging from 200 to 400 °C, the ZnS (1 1 1) diffraction peak was broadened, indicating that a small amount of oxygen had entered the lattice of ZnS:Mn and substituted some S contents. For the thin film annealed at 500 °C, three weak diffraction peaks appeared at $2\theta = 54.3^\circ$, 39.1° and 34.4°, corresponding to the (4 2 1), (3 1 1) directions of $ZnSO_4$ and the (0 0 2) direction of ZnO, respectively, which indicated that ZnS had partially transformed into $ZnSO_4$ and ZnO. With the further increase of annealing temperature, sulfur atoms obtained enough kinetic energy to leave their lattice sites by thermal disturbance and oxygen atoms diffused into the ZnS lattice to occupy the sulfur vacancies. A relative higher annealing temperature also facilitated the formation of stable

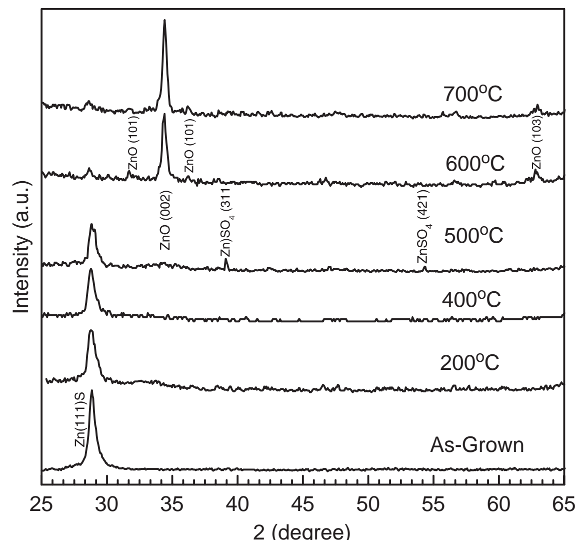

Fig. 1. X-ray diffraction patterns of thin films annealed at different annealing temperatures.

wurtzite structure of ZnO in the thin film [9]. As a result, with increasing the annealing temperature from 500 to 700 °C, the diffraction peaks related to the hexagonal ZnO gradually appeared and sharpened.

Zhang et al. [12] have studied the X-ray photoelectron spectroscopy (XPS) and the electron paramagnetic resonance (EPR) spectra of Mn-passivated ZnO. Their results, especially the asymmetric EPR signal, have confirmed that manganese, which existed as MnO_2, was at or near the surface of nanocrystalline ZnO, forming a core–shell structure of Mn-passivated ZnO [12]. With comparison between the thin films annealed at 600 and 700 °C in Fig. 1, the full-width at half-maximum (FWHM) of ZnO (0 0 2) diffraction peaks were 0.38° and 0.37°, respectively. The FWHM was almost unchanged and implied that MnO_2 that existed at the surface of nanocrystalline ZnO kept the nanocrystalline ZnO from further growth and hence made the mean grain size of ZnO nanocrystalline in thin films unchanged, once the thin film was fully oxidized. Compared with pure ZnO, the (0 0 2) peak position for the thin films annealed at 600 and 700 °C slightly shifted towards smaller diffraction angle. This is because the ion radius of sulfur (1.84 Å) is much larger than that of oxygen (1.32 Å), resulting in an increase of the lattice constant when S impurity entered the ZnO lattice.

Fig. 2 depicts the PL spectra measured at 81.9 K for the thin films annealed at 500, 600 and 700 °C. Each spectrum was composed of an intense near-band-edge emission and a weak deep-level emission band. The weakness of the deep-level emission confirmed that the surface defects of ZnO had been effectively passivated by the capping MnO_2 layer. The inset of Fig. 2 showed an enlargement of the near-band-edge emission for the thin film annealed at 700 °C. The peak located at 3.355 eV was the strongest in the spectrum, which was assigned to the bound exciton emission labeled with I_x. Two shoulders located at around 3.363 and 3.379 eV on the higher energy side were assigned to the bound exciton emission at neutral donors (I_4) and the free exciton emission ($X_{A,B}$), respectively [13,14]. The free exciton emission was accompanied by phonon replicas at 3.310, 3.238 and 3.168 eV [15,16]. The PL spectra for the thin films annealed at 500 and 600 °C had the same features as the film annealed at 700 °C.

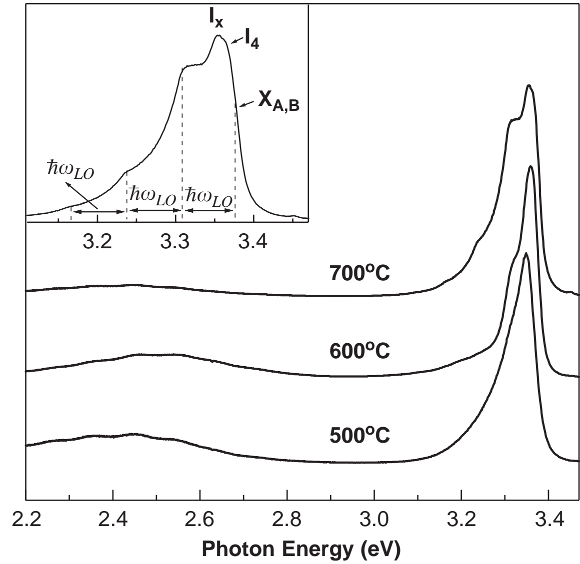

Fig. 2. Photoluminescence spectra measured at 81.9 K for thin films annealed at different temperatures ranging from 500 to 700 °C. The inset shows the enlargement of near-band-edge emission for the thin film annealed at 700 °C.

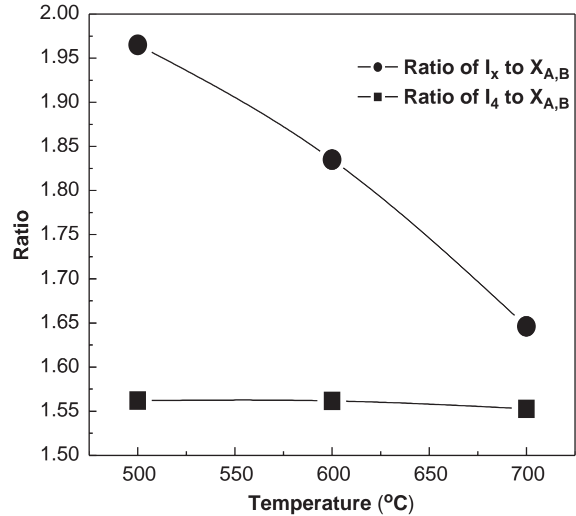

Fig. 3. Intensity ratios of I_x and I_4 to $X_{A,B}$ versus annealing temperature.

The intensity ratios of I_4 and I_x to $X_{A,B}$ versus annealing temperature are given in Fig. 3. Previous

studies have shown that the native defects were mainly presented at the surface of ZnO. Hence, the core–shell structure of MnO_2-capped nanocrystalline ZnO could passivate the intrinsic defects of ZnO, including O vacancies and Zn interstitials [12]. Therefore, the PL intensity of I_4 was expected to show only a slight variation with the annealing temperature. As shown in Fig. 3, the intensity ratio of I_4 to $X_{A,B}$ did not change remarkably as the annealing temperature increased. However, the intensity ratio of I_x to $X_{A,B}$ decreased drastically, which indicated that the exciton bound to I_x did not originate from the intrinsic defects. Combined with XRD data, S content changed in the same way as the intensity ratio of I_x to $X_{A,B}$ changed with increasing annealing temperature. Therefore, we assumed that I_x might originate from excitons bound to S impurity in ZnO. Although S and O are both chalcogens, the different electronegativity and atomic radius can cause a hole isoelectronic trap in the band gap when the sulfur substitutes oxygen in ZnO hosts [17]. The isoelectronic trap bound a hole first by the short-range potential and an electron was subsequently captured via the Coulomb attraction, resulting in the formation of an isoelectronic bound exciton. Therefore, an isoelectronic trap luminescence peak appeared on the low-energy side of I_4 as shown in Fig. 2. With the increasing annealing temperature, the decrease in S content in ZnO by thermal oxidation led to the decrease of the number of isoelectronic bound excitons and the decrease of relative intensity of bound exciton emission related to S. According to the difference between the isoelectronic trap peak position and the free exciton peak position, the estimated binding energy of the isoelectronic bound excitons is 24 meV.

Fig. 4 shows the dependence of the PL spectra of the thin film annealed at 700 °C in the temperature ranging from 81.9 to 302.2 K. As temperature increased, the relative intensity of I_4 and I_x decreased, while the free exciton emission gradually became clearer and eventually dominated the PL spectra at higher temperatures. It was because that the bound excitons were thermally ionized from the donor and sulfur impurities. At the same time, the PL intensity decreased dramatically, mainly due to the increase in the probability of the thermally activated nonradiative recombination process.

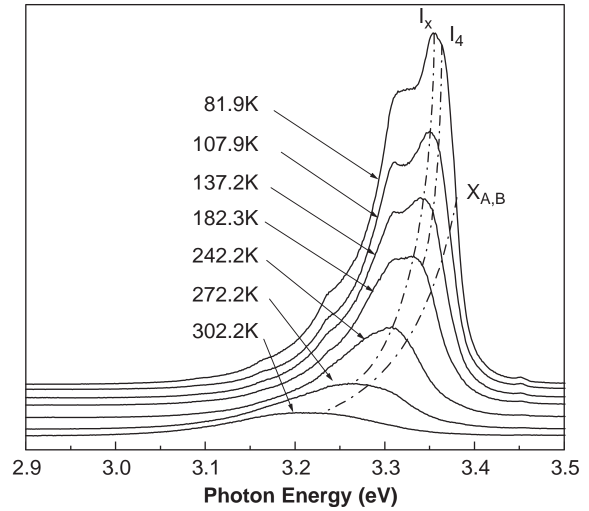

Fig. 4. Dependence of photoluminescence spectra of the thin film annealed at 700 °C on temperature from 82 to 302 K.

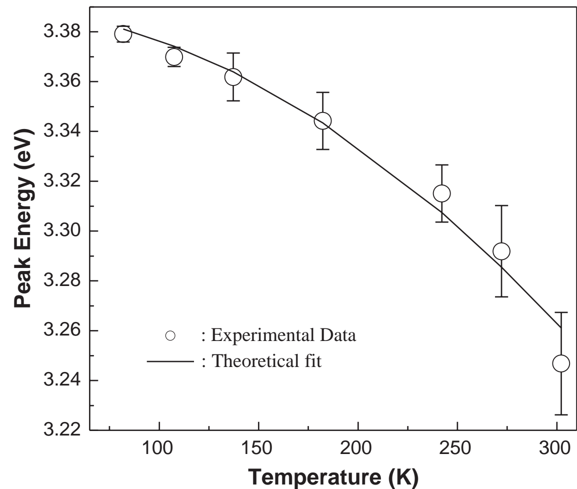

Fig. 5. Free exciton energy as a function of temperature ranging from 81.9 to 302.2 K. The theoretical simulation (solid curve) to the experimental data points (○) is obtained using $E_x(T) = E_x(0) - \alpha T^2/(T+\beta)$.

In order to study the influence of S doping on the band gap energy of ZnO, the peak positions of the observed free exciton emission are plotted versus temperature in Fig. 5. The experimental

data could be fitted to the following formula [14]:

$$E_x(T) = E_x(0) - \alpha T^2/(T + \beta),$$

where $E_x(0)$ is the free exciton energy at 0 K, α represents the $T \to \infty$ limit of the gap entropy $-dE_x(T)/dT$ and β is supposed to be comparable to the Debye temperature of the material. We obtained $E_x(0) = 3.39$ eV. This value was larger than that of the free exciton in pure ZnO (3.37 eV), indicating that doping S in a ZnO film could broaden the optical band gap energy of the ZnO thin film.

Fig. 6 gives the room temperature (RT) PL spectra in the exciton emission region for the thin films annealed at 500, 600 and 700 °C, respectively. The UV emission peak position red-shifted when the annealing temperature increased. This could be explained by the Burstein–Moss effect [18]. When ZnO was doped with S, S impurities could provide the excessive carriers to fill the conduction band edges blocking the low energy transitions and thus widened the optical band gap of ZnO:S. With the increasing annealing temperature, the decrease of S content in the thin film resulted in the decrease of the free carrier density, leading to the redshift of the UV emission peak.

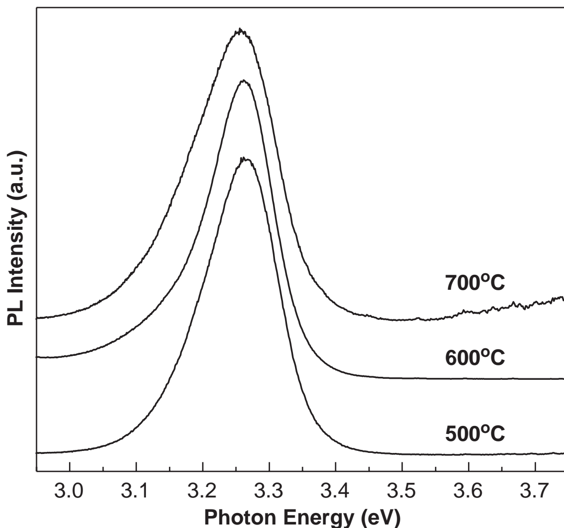

Fig. 6. Room temperature photoluminescence spectra in the excitonic emission region for thin films annealed at temperatures ranging from 500 to 700 °C.

4. Conclusions

The Mn-passivated nanocrystalline ZnO:S thin films were prepared by thermal oxidizing ZnS:Mn films prepared by using electron beam evaporation. The structure and optical properties of the thin films were investigated. Both XRD and PL results showed that doping S into ZnO thin film could be realized when the annealing temperatures reached 600 and 700 °C. S doping widened the optical band gap of ZnO, while the incorporation of Mn in the film passivated effectively the surface defects, simultaneously.

Acknowledgements

This work was supported by the Key Project of National Natural Science Foundation of China under Grant no. 60336020 and the Cultivation Fund of the Key Scientific and Technical Innovation project, Ministry of Education of China (no. 704114).

References

[1] K. Hummer, Phys. Stat. Sol. 56 (1973) 249.
[2] H. Nanto, T. Minami, S. Takata, Phys. Stat. Sol. A 65 (1981) K131.
[3] R.D. Vispute, V. Talyansky, S. Choopun, R.P. Sharma, T. Venkatesan, M. He, X. Tang, J.B. Halpern, M.G. Spencer, Y.X. Li, L.G. Salamanca-Riba, A.A. lliadis, K.A. Jones, Appl. Phys. Lett. 73 (1998) 348.
[4] S. Bethke, H. Pan, B.W. Wesseis, Appl. Phys. Lett. 52 (1988) 138.
[5] Y.F. Chen, D.M. Bagnall, H.J. Koh, K.T. Park, K. Hiraga, Z.Q. Zhu, T. Yao, J. Appl. Phys. 84 (1998) 3912.
[6] Y.Z. Yoo, T. Fukumura, Z. Jin, K. Hasegana, M. Kawasaki, P. Ahmet, T. Chikyow, H. Koinuma, J. Appl. Phys. 90 (2001) 4246.
[7] A. Ohtomo, M. Kawasaki, T. Koida, K. Masubuchi, H. Koinuma, Y. Sakurai, Y. Yoshida, T. Yasuda, Y. Segawa, Appl. Phys. Lett. 72 (1998) 2466.
[8] S. Choopun, R.D. Vispute, W. Yang, R.P. Sharma, T. Venkatesan, H. Shen, Appl. Phys. Lett. 80 (2002) 1529.
[9] Y.Z. Yoo, Y. Osaka, T. Fukumura, Z.W. Jin, M. Kawasaki, H. Koinuma, T. Chikyow, P. Ahmet, A. Setoguchi, S.F. Chichibu, Appl. Phys. Lett. 78 (2001) 616.

[10] Y.Z. Yoo, Z.W. Jin, T. Chikyow, T. Fukumura, M. Kawasaki, H. Koinuma, Appl. Phys. Lett. 81 (2002) 3798.
[11] B.Y. Geng, G.Z. Wang, Z. Jiang, T. Xie, S.H. Sun, G.W. Meng, L.D. Zhang, Appl. Phys. Lett. 82 (2003) 4791.
[12] X.T. Zhang, Y.C. Liu, J.Y. Zhang, Y.M. Lu, D.Z. Shen, X.W. Fan, X.G. Kong, J. Cryst. Growth 254 (2003) 80.
[13] P. Zu, Z.K. Tang, G.K.L. Wong, M. Kawasaki, A. Ohtomo, H. Koinuma, Y. Segawa, Solid State Commun. 103 (1997) 459.
[14] H.J. Ko, Y.F. Chen, Z. Zhu, T. Yao, I. Kobayashi, H. Uchiki, Appl. Phys. Lett. 76 (2000) 1905.
[15] Y. Chen, D.M. Bagnall, Z. Zhu, T. Sekiuchi, K.T. Park, K. Hiraga, T. Yao, S. Koyama, M.Y. Shen, T. Goto, J. Cryst. Growth 181 (1997) 165.
[16] D.M. Bagnall, Y. Chen, M.Y. Shen, Z. Zhu, T. Goto, T. Yao, J. Cryst. Growth 184/185 (1998) 605.
[17] X.R. Xu, M.Z. Su, Luminescence and Luminescent Materials, Chemical Industry Press, China, 2004, p. 105.
[18] K.J. Kim, Y.R. Park, Appl. Phys. Lett. 78 (2001) 475.